JPIChE 49 (2) 2021: 85-93

Journal of Pakistan Institute of Chemical Engineers

journal homepage: www.piche.org.pk/journal

Corrosion Study of Boron Nitride Nanosheets Deposited on Copper Metal by Electrophoretic Deposition

*A. Nadeem, M. A. Raza**

Submitted: 16/08/2021, Accepted: 29/07/2021, Online: 30/12/2021

Abstract

The prime objective of this research is to determine the possibility of corrosion protection offered by boron nitride nanosheets (BNNSs) coated on pure Copper (Cu) strip through electrophoretic deposition (EPD). BNNSs suspension was developed by sonicating hexagonal boron nitride in isopropyl alcohol for 35 h prior to centrifugal partitioning of the supernatant solution, which contained BNNSs having a thickness of ca. 11 nm as shown by atomic force microscopy. BNNSs deposition on the copper substrate was processed in an EPD electrochemical cell arrangement keeping Cu strip as cathode and platinum wire as the anode. The consequent BNNSs coating on the substrate was critically confirmed through a series of microscopies adopting scanning electron, atomic force, and Fourier transform infrared. Energy dispersive x-ray spectroscopy and x-ray diffraction inferred the characterization positively. Tafel analysis and electrochemical impedance spectroscopy both were implied in order to evaluate the anticorrosion performance of coatings developed on substrate copper. The former confirmed an approximate sixfold enhancement in the anti-corrosion capacity of copper protected by BN nanosheets than its bare form. The later, EIS analysis indicated a high impedance and charge transfer resistance ability of BNNSs coatings.

Keywords: Hexagonal boron nitride; Boron nitride nanosheets; centrifugal separation; electrophoretic deposition; electrochemical testing; corrosion protection

1. Introduction:

Two-dimensional nanostructured materials are progressively gaining importance both in academics and industrial sectors due to their superior behaviour such as electrical conductivity, thermal conductivity, oxidation resistance, corrosion and chemical resistance, surface barrier properties, thermal properties, etc. [1-3]. Metallic surfaces, coated with graphene and graphene oxide have presented improved corrosion resistance in the lab studies [4-8]. Despite being promising in refining corrosion resistance of metals, these coatings have been observed to show some situational demerits like raised electrical conductivity and reduced thermal stability [9]. The analogous Boron nitride nanosheets have rather been reported as a suitable substitute that can also mitigate the possibility of galvanic cell formation in between the substrate and the graphene.[10, 11].

Boron nitride (BN), an inorganic ceramic material offers certain inherent useful properties like extended thermal stability, higher stiffness, general chemical inertness, wider optical band gap, elevated thermal conductivity, and stronger UV

[1]*Institute of Metallurgy and Materials Engineering, Faculty of Chemical and Materials Engineering, University of Punjab, Lahore, Pakistan*

Corresponding Author: mohsin.imme@pu.edu.pk

emission [12]. Few layered BNNS with a thickness of 0.414 to 10 nm is known for their high aspect ratio and surface area. These ubiquitous nanosheets have commercially sought-after features of offering high bending modulus (~32 GPa) [13], elevated thermal conductivity (1700–2000 W/mK) [14], and dependable chemical inertness in addition to thermal stability, sometimes even challenging graphene [15]. These nanosheets profoundly exhibit consistent structural properties envisaging lower electrical conductivity, extended thermal shock resistance, impermeability, biofriendly non-toxic behaviour, and a higher dielectric constant [16-19].

Boron nitride nanosheets (BNNSs) because of their novel properties can be picked for multiple expedient utilization. They are used as environmental protective coatings [20], dielectric layers [21], lubricating coatings [22], and hydrophobic coatings [23, 24]. BNNSs also have worthwhile biocompatibility [25]. Their presence as an inorganic reinforcement agent in polymeric and ceramic composites has proven to buttress in overall thermal and mechanical properties [26, 27].

There have been various methods reported to deposit nanomaterials coatings on metallic substrates such as spin coating [28], dip coating —[29], chemical vapor deposition (CVD) [30], and electrophoretic deposition (EPD) [31, 32]. The EPD is found satisfactorily economized and environmentally friendly technique for coatings. CVD has costly operational protocols such as high operating temperature, environment control pressurized gases regulation and complex equipment. Whereas , the surface coatings developed by spin and dip coating techniques need improvement in dependable uniformity and inter-surface adhesion [33].

In the recent past, some researches have reported diversified methods of producing and coating of BNNSs. Husain and coworkers [28] spin coated BNNSs on stainless steel. The corrosion studies showed a solid defensive role of BN films against environmental attack. Sun and his team —[29] dip-coated copper with BNNSs/PVB film to publish that the corrosion inhibition character of this epoxy coating boosted with increased BNNSs proportion in the PVB matrix. He reported his results after performing potentio-dynamic polarization and EIS tests. Ren et al. [34] adopted the CVD route to deposit BNNSs on Cu. Single to several layers of BNNSs were adhered by managing the deposition time. Standard 3.5 % NaCl solution EIS test confirmed betterment in corrosion resistance provided by BNNSs.

The present study shows the successful implication of EPD technique to deposit BNNSs on copper surface reporting its enhanced protection against corrosion. The making and separation of BNNSs were made possible by liquid phase exfoliation /ultrasonication method. Both voltage and time parameters for EPD were optimized to deposit uniform coating. Consequently, the corrosion guarding ability of the resulted coating was electrochemically studied by Tafel analysis and EIS in 3.5 % NaCl solution.

2. Experimental:

2.1. Materials:

Pure Cu strip (99 % purity) was used as a substrate for the deposition of BNNSs by EPD. Isopropanol (IPA) was sourced from Sigma-Aldrich (USA) and h-BN powder (1-2 μm) from US Research Nanomaterials, Inc. respectively.

2.2. Development of BNNSs coating:

The h-BN powder (~125 mg) was dispersed in 125 ml IPA and sonicated for 35 h. The resultant colloidal solution was centrifugated at 4000 rpm for half an hour in the sequential order. The supernatant yield served as the source to develop BNNSs coating on Cu by EPD. In the cell process, Cu strip and platinum were fixed as cathode and anode respectively. To boast the conductivity of supernatant BNNSs solution, 50 μL of HCl was added to suspension. Process diagram for the process setup is sketched as Fig. 1. The coating parameters and deposited mass of BNNSs during EPD process is presented in Table 1. The images of unadorned and BNNSs coated Cu samples are obvious in Fig. 2.

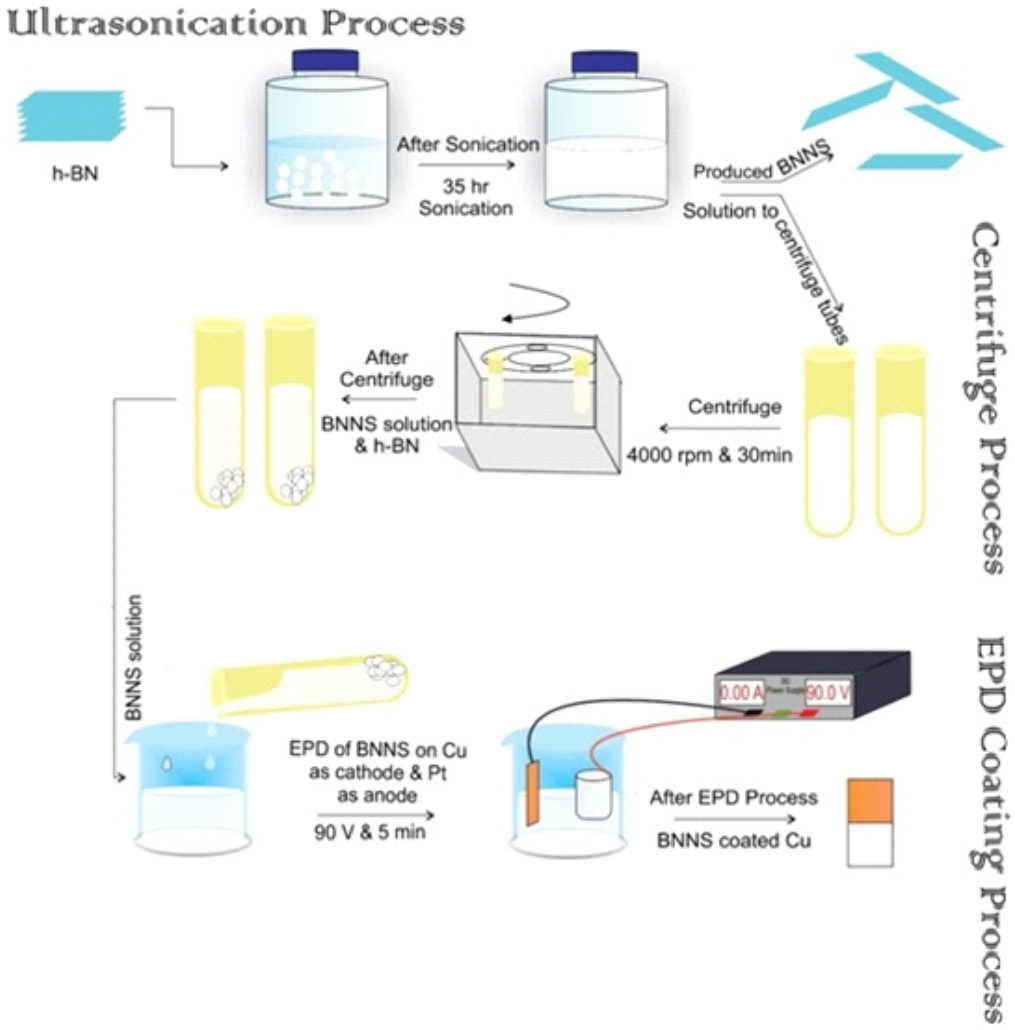

Figure 1: Process setup.

Table 1: Parameters and deposited mass of BNNSs on Cu during EPD process.

Voltage (V)	Deposition time (min)	Deposited mass (mg)
90	1	0.2
90	5	0.4

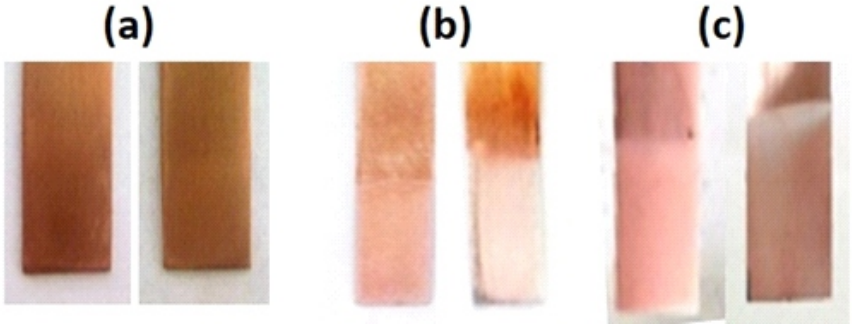

Figure 2: photographs of (a) bare Cu samples, (b) BNNSs coated samples at 90 V for 1 min (deposition time) and (c) BNNSs coated samples at 90 V for 5 min (deposition time)

3. Characterization:

The BNNSs protected Cu samples were characterized for various coating features like structure, roughness, composition, morphology, functionality and corrosion inhibition capability. The thickness and roughness of BNNSs coated Cu sample were deliberated using atomic force microscope [(AFM), NT-MDT, Russia]). Diluted solution of h-BN/ethanol and BNNSs/ethanol suspensions prepared after sonication for 5 min and 30 h, respectively, were drop-casted on mica and images were taken in semi-contact mode. For morphological study, scanning electron microscopy (SEM [Inspect S50, FEI]) was observed on BNNSs and BNNSs-coated Cu. Energy dispersive x-ray spectroscopy powered by EDAX ancillary of SEM with solid state detector was made for a detection window area of 25 mm^2. XRD data was acquired CuKα (λ=0.1546 nm) from 5° to 116°(2θ°). (Equinox 2000, Thermo Scientific). The presence of any functional group associated with BNNSs was analyzed by Fourier transform infrared spectroscopy (FTIR) using (Agilent Cary 630).

Potentiostat/galvanostat/ZRA (Reference 3000, Gamry Instruments, USA) was operated to perform both electrochemical studies; (EIS) and Tafel analysis in a three-electrode cell setup arranging Cu samples as working electrode, platinum wire as counter electrode and saturated calomel electrode (SCE) as reference electrode [35]. For Tafel analysis the potential was applied in anodic and cathodic directions in the range [−0.15 V to 0.15 V (vs. OCP)] with a scanning rate of 0.5 mV/s. For EIS the frequency range applied was 10 mHz to 100 kHz with AC amplitude of ±10 mV(rms) to run through the experiments. Analytical calculations of the generated electrochemical data were processed with the application of software Echem, Analyst version 7.03 (Gamry Instruments, USA).

4. Results and Discussion:

4.1. XRD:

XRD patterns of h-BN and BNNSs-coated Cu sample (5 min deposition time) are better presented in Fig. 3. Magnified pattern of BNNSs-coated Cu shows a distinct peak at 2θ° =26.78° corresponding to the typical (002) peak of BNNSs [36]. This signature peak suggests successful deposition of BNNSs on Cu by EPD. The (002) peak matches the COD data base for h-BN (COD Entry # 96-101-0603). The prominent peaks indexed in BNNSs coated-Cu are due to Cu planes [37].

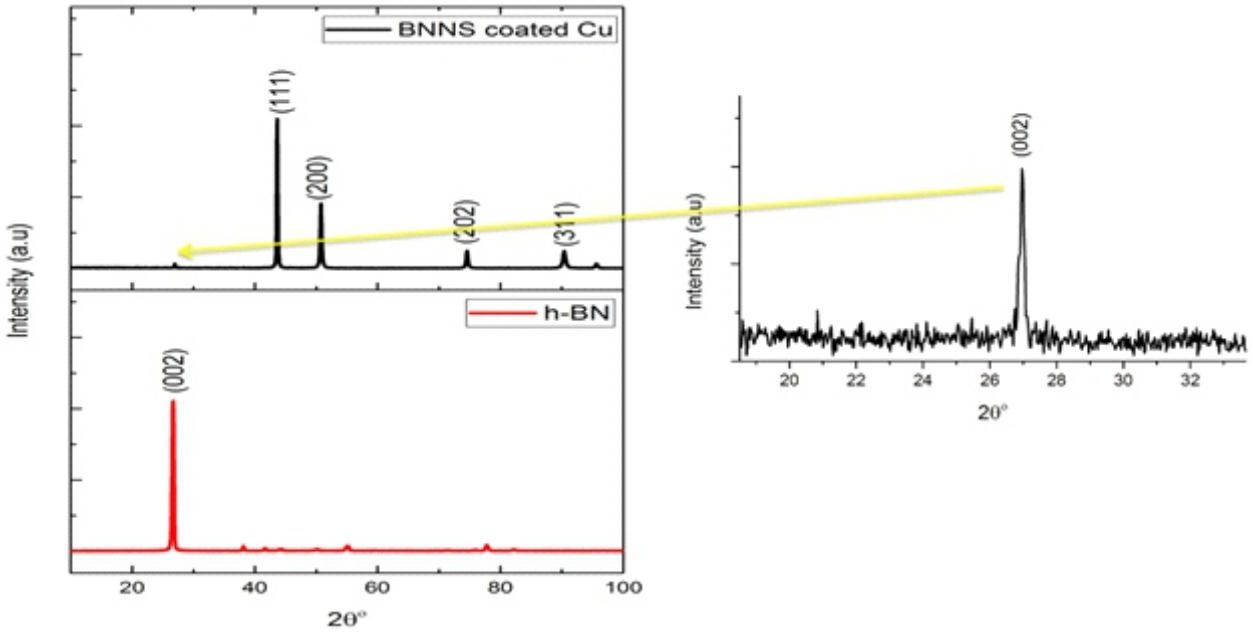

Figure 3: XRD pattern of h-BN (commercial) and BNNSs coated-Cu sample (5 min deposition time)

4.2. FTIR:

FTIR spectra of h-BN and BNNSs-coated Cu sample (5 min deposition) are illustrated in Fig. 4. In this comparison, two noticeable peaks are visible at 760 cm^{-1} and 1330 cm^{-1} which corresponds to sp^2-bonded B-N-B and B-N bending vibrations respectively [38, 39]. Presence of these vibrations in FTIR spectrum of BNNSs-coated Cu confirmed BNNSs deposition on Cu sample. A peak at 3000 cm^{-1} wave number in the coated sample's spectrum witnessed due to presence of –OH groups, which might have resulted due to functionalization of BNNSs during prolonged sonication in IPA.

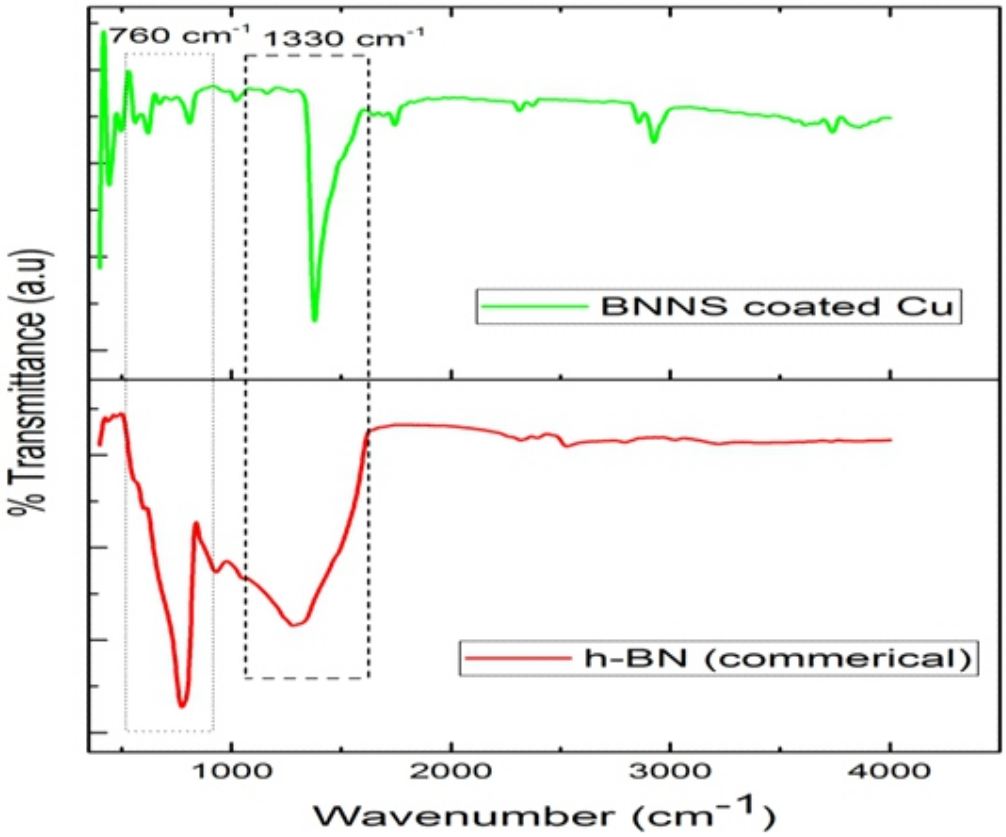

Figure 4: FTIR spectra of h-BN and BNNSs coated-Cu sample (5 min deposition time)

4.3. AFM:

Fig, 5 presents a set of AFM (semi-contact mode) images of h-BN and BNNSs synthesized after a sonication process of 35 hours, BNNSs deposition on copper strip for 5 minutes and also the starting bare copper. Average thickness and lateral dimensions of h-BN being 190 nm and 800 nm, respectively (a), whereas BNNSs produced by sonication have thickness of ca. 11 nm and lateral dimension of ca.220 nm respectively, confirming a definite splitting of h-BN into BNNSs by sonication at the same time.

Table 2 highlights surface roughness of bare Cu and BNNSs coated Cu (5 min deposition) all measured using the same semi-contact mode of AFM. Average Roughness (Ra) of bare Cu was ca.20 nm while BNNSs-coated Cu remained almost 175 nm. BNNSs coated Cu has higher roughness than bare Cu, which might be due to random stacking of BNNSs during deposition summarizes the area coverage of the coatings [40].

Table 2: Roughness of bare vs BNNSs coated Cu (5 min deposition time) samples

Sample	Direction (from center)	Roughness (nm)
Bure Cu	x-axis	20.20
	y-axis	19.85
BNNSs-coated Cu (5 min deposition time)	x-axis	232.0
	y-axis	128.0

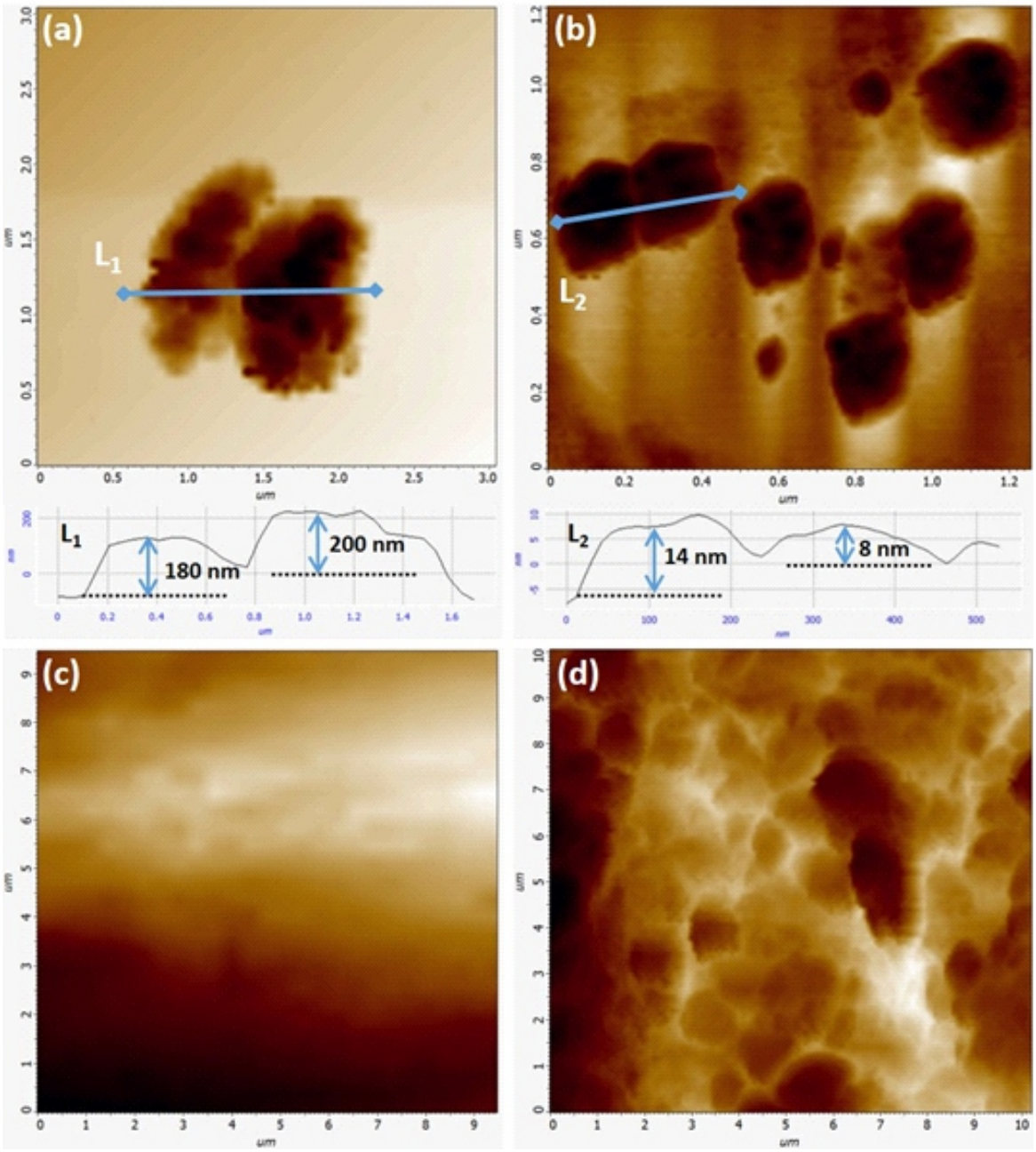

Figure 5: AFM images (a) h-BN, (b) BNNSs produced by sonication (50 h), (c) bare Cu sample and (d) BNNSs -coated Cu sample (5 min deposition time)

4.4. SEM:

SEM and EDX Spectrum of commercial h-BN and BNNSs produced by sonication are shown in Fig. 6 (a & b). SEM shows that the h-BN(a) has large particle size, while BNNSs produced by sonication are smaller flat sheets with average lateral dimensions slightly smaller than h-BN. EDX of h-BN and BNNSs produced by sonication confirms B and N elements in both.

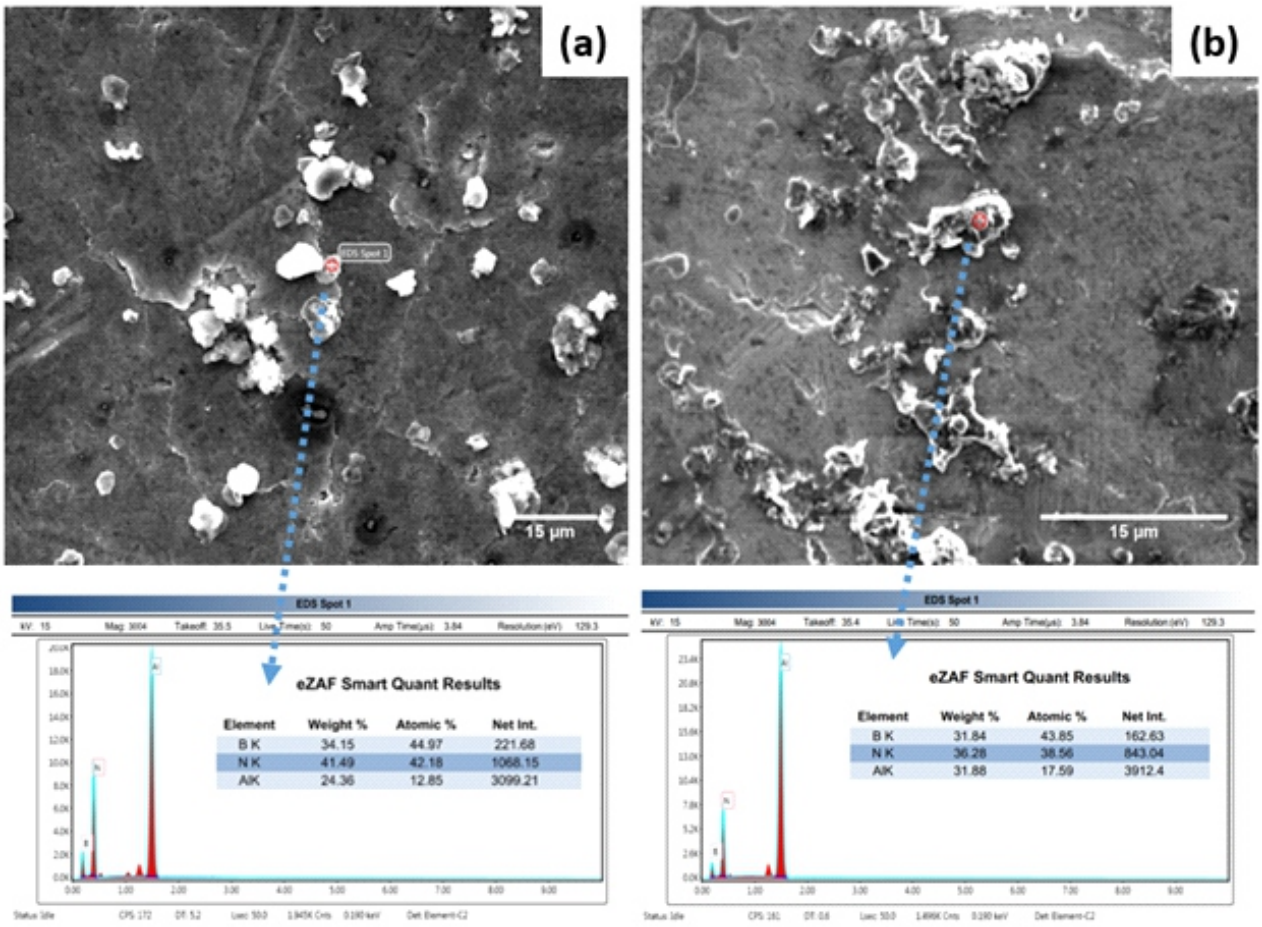

Figure 6: SEM and EDX Spectrum of (a) commercial h-BN and (b) BNNSs produced in IPA by 50 h sonication

SEM image and EDX of BNNSs-coated Cu are presented in Fig. 7. The coated portion of the sample shows uniform coverage of BNNSs and some rougher topography of the coating in agreement with AFM. The high magnification image (Fig. 7) of the coating shows sheets stacked upon one another. The EDX analysis of coated section shows the presence of B, N, and Cu peaks and on uncoated side it indicates only Cu and O peaks. The presence of B and N confirms successful deposition of BNNSs on Cu.

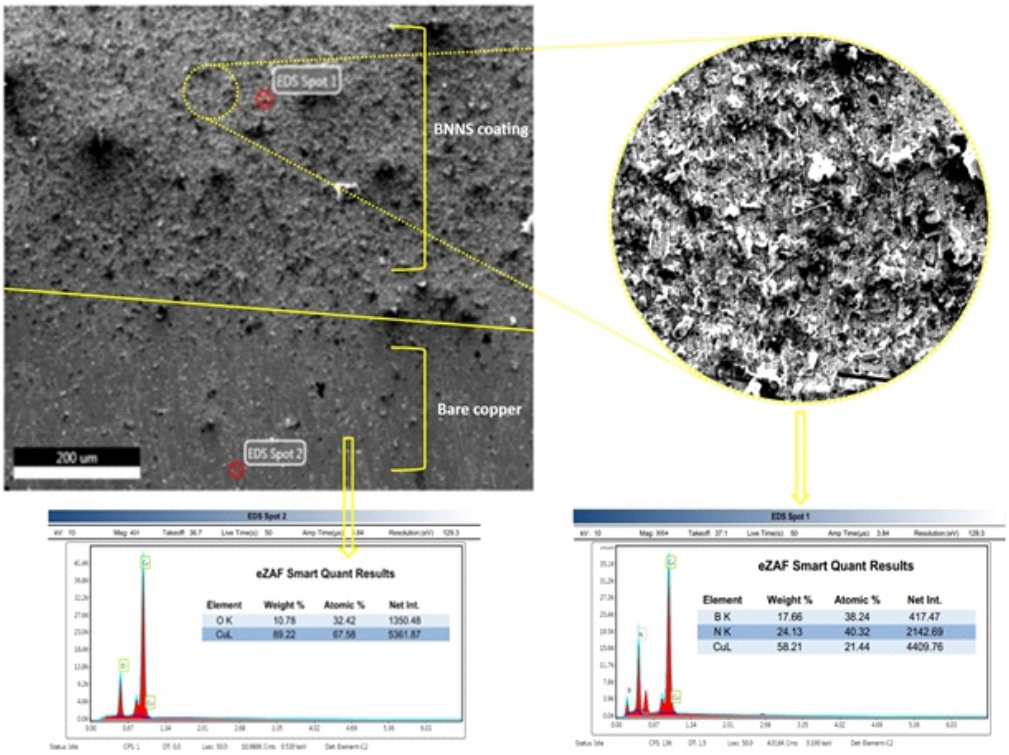

Figure 7: SEM and EDX spectrums of bare Cu and with BNNSs coating (5 min deposition time)

4.5. Electrochemical Testing:

4.5.1. Tafel analysis:

Tafel plots for bare and EPD coated-Cu samples are found drawn in Fig. 8. E_{corr} and Icorr represent corrosion potential and corrosion current respectively. BNNSs EPD-coated samples prepared at 90 V, for 1 min and 90 V, for 5 min are designated as BNNSs-(1) and BNNSs-(5) respectively. Both show a positive shift in Ecorr, the later getting to -185 mV compared to bare Cu (E_{corr}= -230 mV). There is a positive shift of about 45 mV in E_{corr}indicating an improved corrosion resistance. I_{corr} of BNNSs-(5) is decreased to 4.80 μA/cm^{2}as compared to bare Cu (I_{corr} = 21.40 μA/cm^2). BNNSs-(5) sample showed approximately 6 times decrease in corrosion rate compared to bare Cu. Tafel analysis showed that coating deposited at 90 V and 5 min is more resistant to corrosion than what deposited for 1 min. The kinetic data obtained from Tafel curves is presented in Table 3.

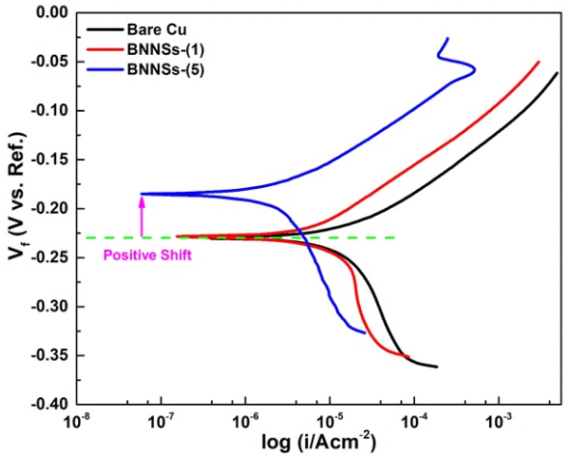

Figure 8: Tafel plotting of bare Cu and BNNSs coated samples at different deposition time duration.

Table 3: Corrosion data of bare Cu and BNNSs-coated Cu

Sample	E_{corr} (mV)	I_{corr} (μA/cm^2)	Corrosion Rate (mpy)
Bare Cu	-230.0	21.40	9.81
BNNSs-(1)	-229.0	11.3	5.86
BNNSs-(5)	-185.0	4.08	1.85

4.5.2. EIS:

EIS was run through to investigate the corrosion mechanism of bare and EPD coated Cu samples. BNNSs-(5) showed better corrosion protection as determined by Tafel analysis. In furtherance, the Nyquist and bode plots for bare and BNNSs-(5) samples indicated that BNNSs-(5) has elevated impedance at higher and lower frequencies compared to bare Cu (Fig.9). Electrical equivalent circuits (EEC) were fitted to calculate related parameters [41]. EEC models are shown in Fig. 10 and the calculated parameter values presented in Table 4. It is clear from these parameters that both $R_{sol(solution\ resistance)}$ and $R_{po\ (polarization\ resistance)}$ of BNNSs-(5) are higher as compared to bare Cu. $R_{ct(charge\ transfer\ resistance)}$, the charge transfer resistance which indicates hinderance towards ion mobilization. Higher R_{ct} of BNNSs-(5) (40.44 kΩ·cm^2) than bare Cu (0.81 kΩ·cm^2) indicates that BNNSs coating deposited by EPD lowers ionic movement which resulted in higher corrosion resistance of BNNSs coated-Cu. Tafel plots are well endorsed by EIS analysis and overall electrochemical characterization showed that BNNSs-(5) Cu sample surely developed enhanced corrosion resistance compared to bare Cu.

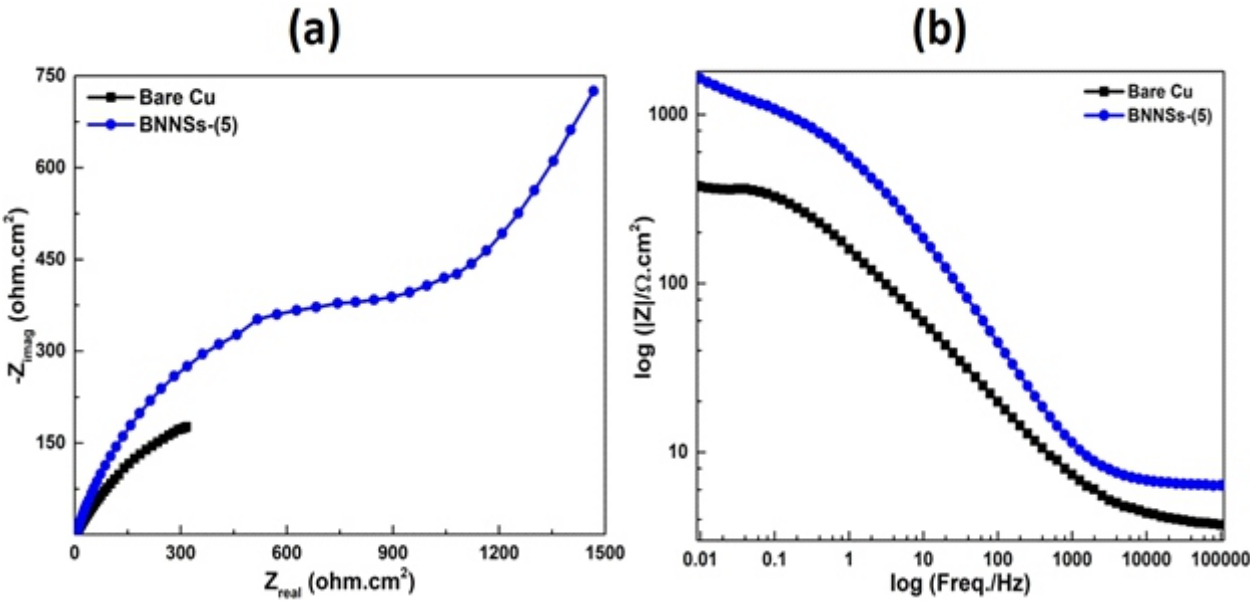

Figure 9: (a) Nyquist and (b) Bode curves of BNNSs-(5) vs Bare Cu samples.

Table 4: EIS parameters obtained using EEC for bare Cu and BNNSs-(5) in 3.5% NaCl

Name	R_{sol} ($\Omega \cdot cm^2$)	R_{po} ($\Omega \cdot cm^2$)	R_{ct} ($k\Omega \cdot cm^2$)	Goodness of fit
Bare Cu	3.213	---	0.81	20.09 E-3
BNNSs-(5)	6.099	614.4	40.44	1.828 E-3

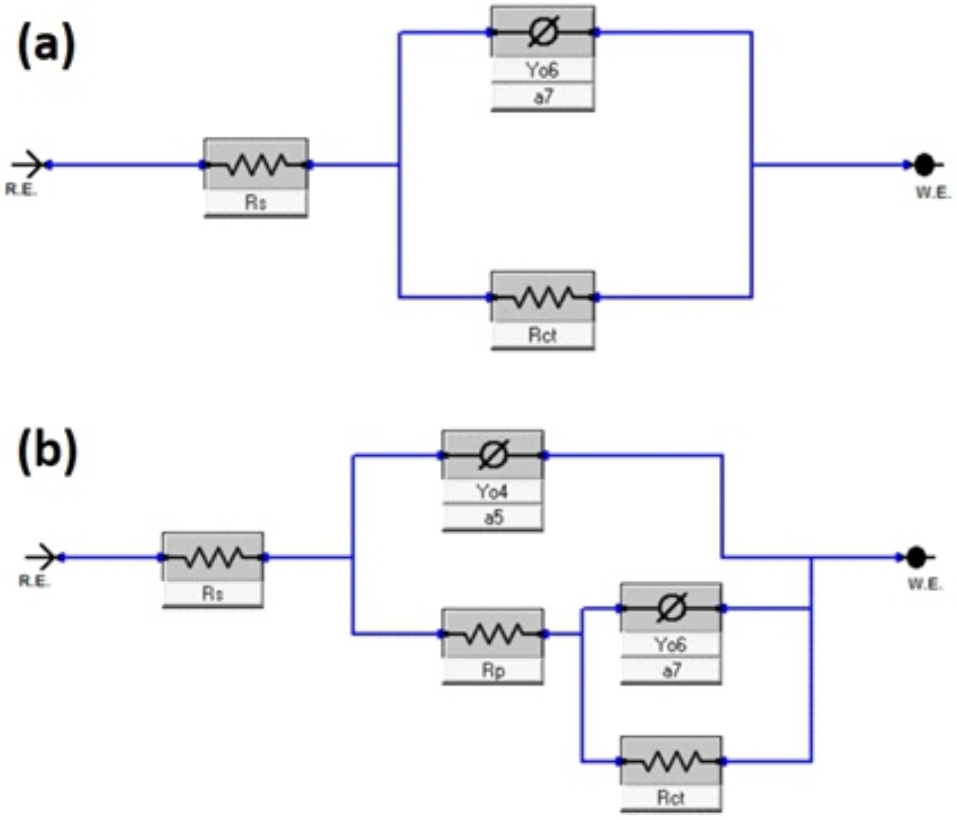

Figure 10: EEC models of (a) Bare Cu and (b) BNNSs coated Cu samples

5. Conclusions:

- BNNSs are successfully synthesized by liquid phase exfoliation method as confirmed by AFM analysis. AFM analysis inferred that BNNSs sheets with thickness of about 11 nm and lateral dimensions of approximately 220 nm were obtained after sonication.
- BNNSs were successfully deposited on Cu substrate as endorsed by FTIR, SEM and AFM analysis.
- Tafel analysis indicated that BNNSs-(5) has improved its corrosion resistance than bare Cu by approximately 6 times.
- EIS analysis confirmed that BNNSs-(5) showed higher R_{ct} in comparison to bare Cu. Tafel results were well validated by EIS analysi

References:

1. S. Chen et al., "Oxidation resistance of graphene-coated Cu and Cu/Ni alloy," ACS nano, vol. 5, no. 2, pp. 1321-1327, 2011.
2. D. Kang et al., "Oxidation resistance of iron and copper foils coated with reduced graphene oxide multilayers," Acs Nano, vol. 6, no. 9, pp. 7763-7769, 2012.
3. R. R. Nair et al., "Fine structure constant defines visual transparency of graphene," Science, vol. 320, no. 5881, pp. 1308-1308, 2008.
4. M. A. Raza, Z. U. Rehman, F. A. Ghauri, A. Ahmad, R. Ahmad, and M. Raffi, "Corrosion study of electrophoretically deposited graphene oxide coatings on copper metal," Thin Solid Films, vol. 620, pp. 150-159, 2016.
5. J. Quezada-Rentería, L. Cházaro-Ruiz, and J. Rangel-Mendez, "Synthesis of reduced graphene oxide (rGO) films onto carbon steel by cathodic electrophoretic deposition: Anticorrosive coating," Carbon, vol. 122, pp. 266-275, 2017.
6. J. H. Park and J. M. Park, "Electrophoretic deposition of graphene oxide on mild carbon steel for anti-corrosion application," Surface and Coatings Technology, vol. 254, pp. 167-174, 2014.
7. M. A. Raza et al., "Electrochemical behavior of graphene coatings deposited on copper metal by electrophoretic deposition and chemical vapor deposition," Surface and Coatings Technology, vol. 332, pp. 112-119, 2017.
8. M. F. Maqsood, M. A. Raza, F. A. Ghauri, Z. U. Rehman, and M. T. Ilyas, "Corrosion study of graphene oxide coatings on AZ31B magnesium alloy," Journal of Coatings Technology and Research, vol. 17, pp. 1321-1329, 2020.
9. J.-H. Ding, H.-R. Zhao, Y. Zheng, X. Zhao, and H.-B. Yu, "A long-term anticorrsive coating through graphene passivation," Carbon, vol. 138, pp. 197-206, 2018.
10. M. Schriver, W. Regan, W. J. Gannett, A. M. Zaniewski, M. F. Crommie, and A. Zettl, "Graphene as a long-term metal oxidation barrier: worse than nothing," ACS nano, vol. 7, no. 7, pp. 5763-5768, 2013.
11. F. Zhou, Z. Li, G. J. Shenoy, L. Li, and H. Liu, "Enhanced room-temperature corrosion of copper in the presence of graphene," Acs Nano, vol. 7, no. 8, pp. 6939-6947, 2013.
12. A. Pakdel, C. Zhi, Y. Bando, and D. Golberg, "Low-dimensional boron nitride nanomaterials," Materials Today, vol. 15, no. 6, pp. 256-265, 2012.
13. C. Li, Y. Bando, C. Zhi, Y. Huang, and D. Golberg, "Thickness-dependent bending modulus of hexagonal boron nitride nanosheets," Nanotechnology, vol. 20, no. 38, p. 385707, 2009.
14. T. Ouyang, Y. Chen, Y. Xie, K. Yang, Z. Bao, and J. Zhong, "Thermal transport in hexagonal boron nitride nanoribbons," Nanotechnology, vol. 21, no. 24, p. 245701, 2010.
15. H. M. Ghassemi, C. H. Lee, Y. K. Yap, and R. S. Yassar, "In situ TEM monitoring of thermal decomposition in individual boron nitride nanotubes," JOM, vol. 62, no. 4, pp. 69-73, 2010.
16. J. Wu et al., "Raman spectroscopy and time-resolved photoluminescence of BN and B x C y N z nanotubes," Nano letters, vol. 4, no. 4, pp. 647-650, 2004.
17. K. Watanabe, T. Taniguchi, and H. Kanda, "Direct-bandgap properties and evidence for ultraviolet lasing of hexagonal boron nitride single crystal," Nature materials, vol. 3, no. 6, p. 404, 2004.
18. Y. Kubota, K. Watanabe, O. Tsuda, and T. Taniguchi, "Deep ultraviolet light-emitting hexagonal boron nitride synthesized at atmospheric pressure," Science, vol. 317, no. 5840, pp. 932-934, 2007.

19. J. MacNaughton et al., "Electronic structure of boron nitride single crystals and films," Physical review B, vol. 72, no. 19, p. 195113, 2005.
20. M. Yi, Z. Shen, X. Zhao, S. Liang, and L. Liu, "Boron nitride nanosheets as oxygen-atom corrosion protective coatings," Applied Physics Letters, vol. 104, no. 14, p. 143101, 2014.
21. H. Fang, S.-L. Bai, and C. P. Wong, "Thermal, mechanical and dielectric properties of flexible BN foam and BN nanosheets reinforced polymer composites for electronic packaging application," Composites Part A: Applied Science and Manufacturing, vol. 100, pp. 71-80, 2017.
22. C. Lee et al., "Frictional characteristics of atomically thin sheets," science, vol. 328, no. 5974, pp. 76-80, 2010.
23. C. R. Dean et al., "Boron nitride substrates for high-quality graphene electronics," Nature nanotechnology, vol. 5, no. 10, p. 722, 2010.
24. A. Pakdel, C. Zhi, Y. Bando, T. Nakayama, and D. Golberg, "Boron nitride nanosheet coatings with controllable water repellency," Acs Nano, vol. 5, no. 8, pp. 6507-6515, 2011.
25. G. Ciofani et al., "A simple approach to covalent functionalization of boron nitride nanotubes," Journal of colloid and interface science, vol. 374, no. 1, pp. 308-314, 2012.
26. X. Liu et al., "Preparation of polyimide composites reinforced with oxygen doped boron nitride nano-sheet as multifunctional materials," Materials & Design, vol. 180, p. 107963, 2019.
27. C. Zhi, Y. Bando, C. Tang, H. Kuwahara, and D. Golberg, "Large scale fabrication of boron nitride nanosheets and their utilization in polymeric composites with improved thermal and mechanical properties," Advanced Materials, vol. 21, no. 28, pp. 2889-2893, 2009.
28. E. Husain, T. N. Narayanan, J. J. Taha-Tijerina, S. Vinod, R. Vajtai, and P. M. Ajayan, "Marine corrosion protective coatings of hexagonal boron nitride thin films on stainless steel," ACS applied materials & interfaces, vol. 5, no. 10, pp. 4129-4135, 2013.
29. W. Sun, L. Wang, T. Wu, Y. Pan, and G. Liu, "Communication—multi-layer boron nitride nanosheets as corrosion-protective coating fillers," Journal of the Electrochemical Society, vol. 163, no. 2, pp. C16-C18, 2016.
30. L. Song et al., "Large scale growth and characterization of atomic hexagonal boron nitride layers," Nano letters, vol. 10, no. 8, pp. 3209-3215, 2010